Universität des Saarlandes

Fachrichtung 6.1 – Mathematik

Preprint

Efficient Algorithms for the Regularization of dynamic inverse Problems - Part I and II

U. Schmitt, A. K. Louis,
C. Wolters and M. Vaukhonen

Preprint No. 45

Saarbrücken 2001

Universität des Saarlandes

Fachrichtung 6.1 – Mathematik

Efficient Algorithms for the Regularization of dynamic inverse Problems - Part I and II

U. Schmitt

Saarland University
Institute for Applied Mathematics
Postfach 15 11 50
D–66041 Saarbrücken
Germany
E-Mail: schmitt@num.uni-sb.de

A. K. Louis

Saarland University
Institute for Applied Mathematics
Postfach 15 11 50
D–66041 Saarbrücken
Germany
E-Mail: louis@num.uni-sb.de

C. Wolters

Max-Planck Institute of
Cognitive Neuroscience
PO Box 500355
D-04303 Leipzig
Germany
E-Mail: wolters@cns.mpg.de

M. Vaukhonen

University of Kuopio
Department of Applied Physics
PO Box 1627
70211 Kuopio
Finland
E-Mail: mvaukhon@messi.uku.fi

submitted: December 18, 2001

Preprint No. 45

Saarbrücken 2001

Edited by
FR 6.1 – Mathematik
Im Stadtwald
D–66041 Saarbrücken
Germany

Fax: + 49 681 302 4443
e-mail: preprint@math.uni-sb.de
WWW: http://www.math.uni-sb.de/

Efficient Algorithms for the Regularization of dynamic inverse Problems – Part I: Theory

U Schmitt and AK Louis

Institute for Applied Mathematics, P.O. Box 151150, Saarland University, 66041 Saarbrücken, Germany.

E-mail: schmitt@num.uni-sb.de

Abstract. In this paper dynamic inverse problems are studied, where the investigated object is allowed to change during the measurement procedure. In order to achieve reasonable results, temporal *a priori* information will be considered. Here, "temporal smoothness" is used as a quite general, but for many applications sufficient, *a priori* information. This is justified in the case of slight movements during a x-ray scan in computerized tomography, or in the field of current density reconstruction, where one wants to conclude from electrical measurements on the heads surface to locations of brain activity.

First, the notion of a dynamic inverse problem is introduced, then we describe how temporal smoothness can be incorporated in the regularization of the problem, and finally an efficient solver and some regularization properties of this solver are presented.

This theory will be exploited in three practically relevant applications in a following paper.

Submitted to: *Inverse Problems*

AMS classification scheme numbers: 34A55, 49N45

1. Introduction

This paper is devoted to the study of dynamic inverse problems, where the object under consideration changes with time during the measuring process.

Starting point is a measuring procedure which needs a certain amount of time. During this time span, single measurements are taken at time steps t_i. Then, a dynamic problem is described by operators A_i, where i is a temporal index. That is, the linear operator A_i maps the properties of an investigated object to the measurements m_i at time step t_i.

Now two cases are considered:

- In the first case, the properties x of the examined object do not change during the measuring process. Thus, we have to solve

$$A_i\, x = y_i \quad \text{for all } i.$$

This is called a *static inverse problem.*

- In the second case, called *dynamic inverse problem*, the examined object is allowed to change during the measuring process, and we have to solve

$$A_i\, x_i = y_i \quad \text{for all } i. \tag{1}$$

Examples for dynamic inverse problems are current density reconstructions based on EEG/MEG measurements [1], dynamic electrical impedance tomography [2], process tomography [3, 4] or x-ray CT where slight patient movements can be detected.

Due to the degree of freedom in (1) and the instability of the problem, *a priori* information has to be considered to achieve reasonable and stable solutions of dynamic inverse problems. This kind of regularization is done by assuming *temporal smoothness* as *a priori* information and is considered by adding a penalty term

$$\sum_i \frac{\|x_{i+1} - x_i\|^2}{(t_{i+1} - t_i)^2}$$

in a suitable norm to the known Tikhonov-Phillips minimization task. An application of this smoothness measure in the context of inverse electrocardiography can be found in [5]. If we try to solve the corresponding minimization problem in a straight-forward manner as in [5], we get to a linear problem which is extremely large and thus too expensive to solve.

Our approach starts in the context of operators between Hilbert spaces and leads to a quite general formulation of our procedure. Discretization, which is needed to achieve implementable algorithms, is done as late as possible. Using this method in part two of this paper, we achieve a new type of temporal CT (computerized tomography) algorithm, which avoids direct discretization of the forward model.

In the following mathematical prerequisites will be supplied and two *efficient* procedures for the solution of dynamic inverse problems are developed. These procedures are formulated in terms of linear operator equations, which we will be discretized by suitable projection schemes. Finally it is observed that in the case of equidistant time steps these procedures are regularizations of the temporally uncoupled respectively of the static problem, depending whether the parameter in front of the penalty term $\sum_i \|x_{i+1} - x_i\|^2$ goes to zero or to infinity.

The temporal inverse problem described above could also be tackled in a statistical context, e.g. by using Kalman-Smoothers or Wiener Filters as proposed in [6]. Our approach introduced above is rather analytical and achieves superior results concerning efficiency: statistical procedures have to consider covariance matrices for each timestep, which are often expensive to compute and are "too large" which affects the efficiency of the procedure. A comparision of these two approaches based on a real world problem, namely temporal impedance tomography, can be found in the second part of this paper. There, we will notice a significant enhancement of speed.

2. The mathematical prerequisites

To set the stage, Hilbert spaces H and G_i and linear operators $A_i \in \mathcal{L}(H, G_i)$ are considered. The operator A_i maps the properties $x \in H$ of an examined object to measurements $y_i \in G_i$. The H and G_i are equipped with norms $\|\cdot\|_H$ and $\|\cdot\|_{G_i}$ and scalar products $\langle\cdot,\cdot\rangle_H$ and $\langle\cdot,\cdot\rangle_{G_i}$. These space related indices will be omitted in most cases if they are determined by their context. As the operators A_i all together are assumed to determine a static x sufficiently, the single A_i are in most cases *under-determined*. An operator A is called "under-determined" if

- A is a matrix over $\mathbb{K}$, which has more columns than rows,
- A maps from an infinite-dimensional Hilbert space to $\mathbb{K}^n$, or
- A maps from a function space over a manifold to a function space over a less-dimensional manifold. In the context of Sobolev spaces this can be stated as $A : H^s(M_1) \to H^t(M_2)$ and $\dim M_1 > \dim M_2$.

$\mathbb{K}$ means either the real field or the complex field.

These operators have the property that equations of the form $AA^*u = y$ are easier or cheaper to solve (maybe numerically) than equations like $A^*Ax = A^*y$.

Definition 2.1 Given A_i, x, y_i as above, $x_i \in H$, we call

$$A_i\, x = y_i \quad \text{for all } i$$

a *static problem*, and

$$A_i\, x_i = y_i \quad \text{for all } i$$

a *dynamic problem*.

For the further steps we need the following definition.

Definition 2.2 The *Hilbert space sum* $H_1 \oplus \cdots \oplus H_n$ is the set $H_1 \times \cdots \times H_n$ equipped with the scalar product

$$\langle x, y\rangle := \sum_i \langle x_i, y_i\rangle_{H_i}.$$

The associated norm is defined accordingly.

Definition 2.3 An *operator matrix* is a collection of operators $A_{i,j} : G_j \to H_i, 1 \le i \le n, 1 \le j \le m$. These matrices can be multiplied by

$$(A \cdot B)_{i,j} = \sum_k A_{i,k} B_{k,j},$$

provided that the involved operators match. Addition of operator matrices is done entry by entry. To such a matrix we can assign an linear operator

$$[A] : G_1 \oplus \cdots \oplus G_m \to H_1 \oplus \cdots \oplus H_n$$

by

$$([A]x)_i = \sum_{j=1}^{m} A_{i,j} x_j.$$

The next theorem is important for the following calculations

Theorem 2.4 The map $A \mapsto [A]$ is an isomorphism between the set of operator matrices and the set of the linear operators $\mathcal{L}(H_1 \oplus \cdots \oplus H_n, G_1 \oplus \cdots \oplus G_m)$ according to $[A] \circ [B] = [A \cdot B]$ and $[A] + [B] = [A + B]$.

Proof: Most steps of the proof are easy. We only want to show that the considered map is surjective: for a given operator $B \in \mathcal{L}(H_1 \oplus \cdots \oplus H_n, G_1 \oplus \cdots \oplus G_m)$ we define the operator matrix

$$A_{i,j} = P_i B E_j$$

with canonical projections

$$P_i : H_1 \oplus \cdots \oplus H_n \to H_i$$

and canonical embeddings

$$E_j : H_j \to H_1 \oplus \cdots \oplus H_n.$$

Now it is easy to show $[A] = B$. ■

This theorem allows to calculate with operator matrices and operators which are assigned to operator matrices in the same way as with the well known matrices about fields. This includes that block matrices can be multiplied block wise, see [7], and that one needs not to distinguish between a matrix of operators and the assigned linear operator.

Furthermore the known Kronecker product of matrices [7] can be extended in the following way

Definition 2.5 Let M be a matrix in $\mathbb{K}^{n\times m}$ and B an linear operator $B : H \to G$. Then the *generalized Kronecker product* $M \otimes B$ is the operator

$$M \otimes B = \begin{bmatrix} m_{1,1}B & \cdots & m_{1,m}B \\ \vdots & & \vdots \\ m_{n,1}B & \cdots & m_{n,m}B \end{bmatrix}.$$

The following properties are easy to show:

$$\begin{aligned} (M \otimes A)(N \otimes B) &= (MN) \otimes (AB) \\ (M \otimes A)^{-1} &= M^{-1} \otimes A^{-1} \\ (M \otimes B)^* &= M^* \otimes B^* \end{aligned}$$

Furthermore $\otimes$ and $+$ are distributive, $\otimes$ is associative.

For simplifying the solution process of equations of the type

$$\sum_{i=1}^{T} (M_i \otimes A_i)\, x = y$$

in the special case that the A_i are matrices over a filed $\mathbb{K}$, the following theorem is quite useful. First we have to give a definition:

Definition 2.6 Suppose $x \in \mathbb{K}^{nm}$. Then define the rearrangement

$$\mathrm{Mat}_n(x) = X := \begin{pmatrix} x_1 & x_{1+n} & \cdots & x_{1+(m-1)n} \\ x_2 & x_{2+n} & \cdots & x_{2+(m-1)n} \\ \vdots & & & \vdots \\ x_n & x_{2n} & \cdots & x_{mn} \end{pmatrix}.$$

Now the following theorem can be stated. The proof is easy and therefore omitted.

Theorem 2.7 Given $M_i \in \mathbb{K}^{n\times n}, A_i \in \mathbb{K}^{m\times m}, 1 \le i \le T$ and $x, y \in \mathbb{K}^{nm}$, $X = \mathrm{Mat}_n(x)$ and $Y = \mathrm{Mat}_n(y)$, then the equation

$$\sum_{i=1}^{T} (M_i \otimes A_i)\, x = y$$

is equivalent to the matrix equation

$$\sum_{i=1}^{T} A_i X M_i^\top = Y.$$

Equations of the type $AXB^\top + CXD^\top = Y$ are called *generalized Sylvester equations* and can be solved much more efficiently than the equivalent Kronecker type equation $(A \otimes B + C \otimes D)\, x = y$; see [8].

For the further calculations we need another Lemma, it is about the solution of the so called Tikhonov-Phillips minimization problem:

Lemma 2.8 Given linear operators $A : H \to G_1, B : H \to G_2$ between Hilbert spaces H and G_1, G_2 respectively, such that B^*B is positive definitive. Furhermore let $x \in H, y \in G_1$ and $\lambda \in \mathbb{R}, \lambda \neq 0$. The unique solution of the minimization task

$$\|A\,x - y\|^2 + \lambda^2 \|B\,x\|^2 \to \min$$

can be determined by solving

$$(A^*A + \lambda^2 B^*B)\, x = A^* y. \tag{2}$$

If we have the relation

$$B^*BA = A^*E \tag{3}$$

for a positive definite $E : G_1 \to G_2$, equation (2) is equivalent to solving

$$(AA^* + \lambda^2 E)\, u = y \tag{4}$$

and setting $x = A^*u$.

Proof: Due to $\lambda \neq 0$ the functional $\Phi(x) = \|A\,x - y\|^2 + \lambda^2 \|B\,x\|^2$ is strictly convex. So this functional has a unique solution, which can be achieved by solving $D\Phi(x) = 0$ where $D\Phi$ is the Frechet derivative of Φ. If we take into account that $DF(x)$ of $F(x) = \|A\,x - y\|^2$ fulfills We define $DF(x)\,h = 2\langle A^*(A\,x - y), h\rangle$, we get the linear equation stated above. The last statement is true because of

$$(A^*A + \lambda^2 B^*B)^{-1} A^* = A^* (AA^* + \lambda^2 E)^{-1}.$$

If A is under-determined, the last equation is easier respectivly cheaper to solve than the first one.

3. The procedure STR

In the following three procedures which can be used to solve dynamic inverse problems under the consideration of temporal smoothness as *a priori* information are presented. The first one, called normal equation approach, is not very efficient in the case of under-determined forward operators. Therefore a more efficient procedure called STR (=Spatio Temporal Regularizer) will be derived.

We start with linear operators $A_i, 1 \leq i \leq T$, which map the dynamic solutions x_i to measurements y_i. Further, it is supposed that the A_i either are compact operators between infinite-dimensional Hilbert spaces or are ill-conditioned matrices.

In order to solve the dynamic problem, we start with the minimization problem

$$\Phi(x) = \sum_{i=1}^{T} \|A_i x_i - y_i\|^2 + \lambda^2 \sum_{i=1}^{T} \|x_i\|^2 + \mu^2 \sum_i \frac{\|x_{i+1} - x_i\|^2}{(t_{i+1} - t_i)^2} \to \min. \tag{5}$$

Minimization of the first term forces compliance with the relation $A_i\, x_i = y_i$ for all i. The second term is of the type "spatial Tikhonov-Phillips-Regularization" and the third term measures the temporal smoothness of the x_i.

The following notations are introduced

$$\begin{aligned}
H^T &= H \oplus \cdots \oplus H \quad \text{(T times)} \\
A &= \operatorname{diag}(A_i) \in \mathcal{L}(H^T, G_1 \oplus \cdots \oplus G_T) \\
x &= (x_1, \ldots, x_T)^\top \in H^T \\
y &= (y_1, \ldots, y_T)^\top \in G_1 \oplus \cdots \oplus G_T \\
B &= D \otimes I_H \in \mathcal{L}(H^T, H^{T-1}) \\
D &= \begin{pmatrix}
\frac{1}{t_2 - t_1} & -\frac{1}{t_2 - t_1} & & \\
 & \frac{1}{t_3 - t_2} & -\frac{1}{t_3 - t_2} & \\
 & & \ddots & \ddots \\
 & & & \frac{1}{t_T - t_{T-1}} \quad -\frac{1}{t_T - t_{T-1}}
\end{pmatrix} \in \mathbb{R}^{T \times (T-1)}.
\end{aligned}$$

One could use other forms of D. For example, if we assume equidistant timesteps $t_i = i$, $D = (-\delta_{i,j+1} + 2\delta_{i,j} - \delta_{i,j-1})_{i,j}$ leads to second order temporal smoothness of the x_i.

Now, the functional in (5) can be rewritten as

$$\Phi(x) = \|A\, x - y\|^2 + \lambda^2 \|x\|^2 + \mu^2 \|B\, x\|^2 \to \min.$$

As this functional is strict convex, a minimum exists, which is achieved by solving $D\Phi(x) = 0$. This derivative can be calculated according to the derivative occurring in the proof of Lemma 2.8, and we get the *normal equation*

$$(A^* A + \lambda^2 I + \mu^2 B^* B)\, x = A^*\, y. \tag{6}$$

As the A_i are under-determined this is a "quite large" problem. Unfortunately the technique used in the proof of Lemma 2.8 does not work here, a relation like (3) is not valid in this case. Thus, another technique must be used to achieve an efficient procedure, involving "small" operators $A_i A_j^*$.

Starting point for an efficient procedure involving operator matrices with entries $A_i A_j^*$ is the following minimization problem which is equivalent to (5): One solves

$$\Phi(x, d) = \sum_{i=1}^{T} \|A_i x_i - y_i\|^2 + \lambda^2 \sum_{i=1}^{T} \|x_i\|^2 + \mu^2 \sum_{i=1}^{T-1} \|d_i\|^2 \to \min \tag{7}$$

in connection with the constraints

$$d_i = (x_{i+1} - x_i)/(t_{i+1} - t_i). \tag{8}$$

In order to solve the minimization problem above, these constraints are coupled to the functional Φ by adding a penalty term. That is, we get solutions x_α of

$$\Phi_\alpha(x,d) = \sum_{i=1}^{T} \|A_i x_i - y_i\|^2 + \lambda^2 \sum_{i=1}^{T} \|x_i\|^2 + \mu^2 \sum_{i=1}^{T} \|d_i\|^2 + \alpha^2 \sum_{i=1}^{T} \left\| d_i - \frac{x_{i+1} - x_i}{t_{i+1} - t_i} \right\|^2 \to \min \tag{9}$$

and achieve the solution x of (7), (8) by

$$x = \lim_{\alpha \to \infty} x_\alpha.$$

If d_i is scaled as $d_i = \lambda/\mu\, \delta_i$, and if the following notion is used

$$\delta = (\delta_1, \ldots, \delta_{T-1})^\top \in H^{T-1},$$

the minimization problem (9) can be written as

$$\left\| \underbrace{\begin{bmatrix} A & 0 \\ \alpha B & \alpha \frac{\lambda}{\mu} I \end{bmatrix}}_{M_\alpha} \begin{pmatrix} x \\ \delta \end{pmatrix} - \begin{pmatrix} y \\ 0 \end{pmatrix} \right\|^2 + \lambda^2 \left\| \begin{pmatrix} x \\ \delta \end{pmatrix} \right\|^2 \to \min .$$

This is a Tikhonov-Phillips problem which can be solved as stated in Lemma 2.8:

$$\begin{pmatrix} x^\alpha \\ \delta^\alpha \end{pmatrix} = M_\alpha^* \left(M_\alpha M_\alpha^* + \lambda^2 I \right)^{-1} \begin{pmatrix} y \\ 0 \end{pmatrix}. \tag{10}$$

In order to determine x^α, first the following equation

$$\left(M_\alpha M_\alpha^* + \lambda^2 I \right) \begin{pmatrix} u \\ v \end{pmatrix} = \begin{pmatrix} y \\ 0 \end{pmatrix}.$$

is solved. We have

$$M_\alpha M_\alpha^* + \lambda^2 I = \begin{bmatrix} AA^* & \alpha AB^* \\ \alpha BA^* & \alpha^2 (BB^* + \frac{\lambda^2}{\mu^2} I) \end{bmatrix} + \lambda^2 I.$$

Thus, one has to solve

$$AA^*\, u + \alpha AB^* v + \lambda^2\, u = y \tag{11}$$

$$\alpha BA^*\, u + \alpha^2 (BB^* + \frac{\lambda^2}{\mu^2} I)\, v + \lambda^2\, v = 0. \tag{12}$$

v can be calculated from (12) as

$$v = -\frac{1}{\alpha} \left(BB^* + \left(\frac{\lambda^2}{\mu^2} + \frac{\lambda^2}{\alpha^2} \right) I \right)^{-1} BA^*\, u. \tag{13}$$

Substituted in (11), the following equation for u is achieved :

$$A \Big(I - \underbrace{B^* \left(BB^* + \left(\frac{\lambda^2}{\mu^2} + \frac{\lambda^2}{\alpha^2} \right) I \right)^{-1} B}_{N^\alpha} \Big) A^*\, u + \lambda^2\, u = y. \tag{14}$$

N^α can be simplified to

$$\begin{aligned} N^\alpha &= (D^\top \otimes I_H)\left[(D\otimes I_H)(D^\top I_H) + \left(\frac{\lambda^2}{\mu^2}+\frac{\lambda^2}{\alpha^2}\right)(I_{T-1}\otimes I_H)\right]^{-1}(D\otimes I_H) \\ &= (D^\top \otimes I_H)\Bigg[\underbrace{\left(DD^\top + \left(\frac{\lambda^2}{\mu^2}+\frac{\lambda^2}{\alpha^2}\right) I_{T-1}\right)^{-1}}_{Q^\alpha} \otimes I_H\Bigg](D\otimes I_H) \\ &= (D^\top Q^\alpha D)\otimes I_H. \end{aligned}$$

Then, (14) is equivalent to

$$A\left[I_T\otimes I_H - (D^\top Q^\alpha D)\otimes I_H\right] A^* u + \lambda^2 u = y,$$

respectively

$$A\Bigg(\big(\underbrace{I_T - D^\top Q^\alpha D}_{R^\alpha}\big)\otimes I_H\Bigg) A^* u + \lambda^2 u = y.$$

So we define

$$C^\alpha := A(R^\alpha \otimes I_H)A^* = \left[r^\alpha_{i,j} A_i A_j^*\right]_{i,j},$$

and

$$(C^\alpha + \lambda^2 I_{G_1\oplus\cdots\oplus G_T})\, u = y \tag{15}$$

has to be solved. If we consider (13), an analogous calculation yields

$$v = -\frac{1}{\alpha}\left[(Q^\alpha D)\otimes I_H\right] A^* u.$$

Because of (10) one gets

$$\begin{pmatrix} x^\alpha \\ r^\alpha \end{pmatrix} = M^*_\alpha \begin{pmatrix} u \\ v \end{pmatrix},$$

which supplies

$$\begin{aligned} x^\alpha &= A^* u - B^*\left[(Q^\alpha D)\otimes I_H\right] A^* u \\ &= \left[R^\alpha \otimes I_H\right] A^* u. \end{aligned}$$

Finally, one gets the following procedure for calculating x^α: First solve

$$(C^\alpha + \lambda^2 I_{G_1\oplus\cdots\oplus G_T})\, u = y,$$

then put

$$x^\alpha = \left[R^\alpha \otimes I_H\right] A^* u.$$

The last step to achieve a solution x of (7), (8) is to perform the process $\alpha\to\infty$: from (15) we get the equation

$$(C + \lambda^2 I_{G_1\oplus\cdots\oplus G_T})\, u = y$$

with

$$C = \lim_{\alpha\to\infty} C^\alpha = A\,(\lim_{\alpha\to\infty} R^\alpha)A^* = ARA^*,$$

whereas

$$\begin{aligned} R &= I_T - D^\top Q D \\ Q &= \left(DD^\top + \frac{\lambda^2}{\mu^2} I_{T-1}\right)^{-1}. \end{aligned} \tag{16}$$

So one gets the solution x of (7), (8) by

$$x = \lim_{\alpha \to \infty} x^\alpha = (R \otimes I_H) A^* u. \tag{17}$$

That is

$$x_i = \sum_j r_{i,j} A_j^* u_j.$$

If the calculations above are summarized, we get the following procedure STR for the solution of (5):

(i) **Input**: data y, spatial regularization parameter λ, temporal regularization parameter μ.

(ii) Calculate Q and R according to (16)

$$Q = \left(DD^\top + \frac{\lambda^2}{\mu^2} I_{T-1} \right)^{-1}$$
$$R = I_T - D^\top Q D = (r_{i,j})_{i,j}.$$

(iii) C is defined by

$$C = [r_{i,j} A_i A_j^*]_{i,j}.$$

(iv) Solve

$$(C + \lambda^2 I_{G_1 \oplus \cdots \oplus G_T})\, u = y.$$

(v) Finally, calculate the x_i by

$$x_i = \sum_j r_{i,j} A_j^* u_j.$$

In order to achieve efficiency, in a first step one calculates $A_j^* u_j$ for each j and afterwards x_i.

The procedure presented above involves "small" operators $A_i A_j^*$ which leads to the announced efficiency compared to (6). Statistical procedures as the Kalman-filter which will be introduced in the second part of this paper, result in linear equations in terms of $A_i C_i A_i^*$. These are as "small" as the operators in the procedure above but are in most cases expensive to compute due to the size of the appearing C_i.

As the linear operator C may be an operator between infinite dimensional Hilbert spaces, the procedure above *is not an algorithm.* In order to get an algorithm the operator equation in step (iv) must be solved numerically for instance by a projection scheme. In the next section it is explained how a projection scheme works, and then how such a scheme can be applied in order to approximate the solution of the equation in step (iv). In the end, an efficient algorithm for the numerical stable solution of dynamic inverse problems is achieved.

4. Solving operator matrix equations by projection schemes

Here we give a short description how projection schemes work and how we can apply them to the operator matrix equation emerging in procedure STR. More detailed

information about projection schemes, especially convergence theorems can be found in [10].

Given are Banach spaces X, Y and a linear, continuous and injective operator $T : X \to Y$. The operator equation $T\,x = y$ is considered. In order to calculate an approximative solution, one searches x_h in an finite dimensional subspace X_h of X such that

$$\Psi T\, x_h = \Psi y \qquad \text{for all} \quad \Psi \in Y_h^*.$$

Here Y_h^* is a finite dimensional subspace of Y^*. If it is assumed that $X_h = \text{span}\{\phi_1, \ldots, \phi_n\}$ and $Y_h^* = \text{span}\{\psi_1, \ldots, \psi_n\}$, one gets x_h as

$$x_h = \sum_{i=1}^{n} \alpha_i \phi_i,$$

where α fulfills

$$T_h\, \alpha = y_h.$$

Here $(T_h)_{i,j} = \psi_i T \phi_j$ and $(y_h)_i = \psi_i y$.

Now, we can describe how to achieve a projection scheme in case of an operator matrix $T = [C]$. We start from linear operators $C_{i,j} : H_j \to G_i$ with Banach spaces $G_i, H_j, 1 \le i, j \le n$. The spaces H_i are approximated by

$$H_i^h = \text{span}\{\phi_{i,j} \,|\, 1 \le j \le m_i\} \subset H_i.$$

As functionals in G_i we have

$$(G_i^*)^h = \text{span}\{\psi_{i,j} \,|\, 1 \le j \le n_i\} \subset G_i^*.$$

Now the operator equation

$$[C] f = g$$

with

$$[C] : \underbrace{H_1 \times \cdots \times H_m}_{H} \to \underbrace{G_1 \times \cdots \times G_n}_{G}$$

will be considered. Starting from the given subspaces H_i^h and $(G_i^*)^h$, the subspaces H^h and $(G^*)^h$ are constructed as follows. We define

$$p(i,j) = \sum_{l=1}^{i-1} n_l + j \quad \text{and} \quad q(i,j) = \sum_{l=1}^{i-1} m_l + j.$$

p maps $\{(i,j) \,|\, 1 \le i \le n, 1 \le j \le m_i\}$ bijectively to $\{1 \ldots \sum m_i\}$. q has an analogous property. Now one uses

$$\Phi_{q(i,j)} = (0, \ldots, \underbrace{\phi_{i,j}}_{i\text{–th place}}, \ldots, 0)$$

as a basis of a finite dimensional subspace H^h of H and

$$\Psi_{p(i,j)}(y_1, \ldots, y_n) = \psi_{i,j}(y_i)$$

as testing functionals in G^*. In other words:

$$H^h = \text{span}\{\Phi_l \,|\, 1 \le l \le \textstyle\sum m_i\} \quad \text{and} \quad (G^*)^h = \text{span}\{\Psi_l \,|\, 1 \le l \le \textstyle\sum n_i\}$$

are chosen.

Finally, the matrix D as a discretization of $[C]$ and $B_{i,j}$ as a discretization of $C_{i,j}$ are constructed. That is

$$D_{i,j} = \Psi_i [C] \Phi_j \quad \text{and} \quad (B_{i,j})_{k,l} = \psi_{i,k} C_{i,j} \phi_{j,l}.$$

Then we have

Lemma 4.1 The discretization D of $[C]$ can be constructed from the discretizations $B_{i,j}$ of $C_{i,j}$ by block wise compounding.

Proof: We have

$$\begin{aligned} D_{p(i,k),q(j,l)} &= \Psi_{p(i,k)}[C]\Phi_{q(j,l)} = \Psi_{p(i,k)}(C_{1,j}\phi_{j,l}, C_{2,j}\phi_{j,l}, \dots C_{n,j}\phi_{j,l}) \\ &= \psi_{i,k}C_{i,j}\phi_{j,l} = (B_{i,j})_{k,l}. \end{aligned}$$

■

Now we know how to solve step (iv) in the procedure STR numerically, and we get an efficient algorithm for the solution of dynamic inverse problems.

5. The procedure STR-C

In some applications, e.g. current density reconstruction, the operators A_i are not depending on i, that is $A_i = A_0$ for all i. In this case, the operator C is

$$C = [r_{i,j}A_0A_0^*] = R \otimes (A_0A_0^*).$$

If A_0 additionally is a matrix of size $n \times N$ we get according to Theorem **??**, equation (17) and the relation $A^* = I_T \otimes A_0^*$ the following procedure STR-C ('C' means 'Constant operator'):

(i) **Input**: data y, spatial regularization parameter λ, temporal regularization parameter μ.

(ii) Calculate Q and R according to

$$\begin{aligned} Q &= \left(DD^\top + \frac{\lambda^2}{\mu^2}I_{T-1}\right)^{-1} \\ R &= I_T - D^\top QD. \end{aligned}$$

(iii) Solve the generalized Sylvester equation

$$(A_0A_0^*)UR + \lambda^2 U = \mathrm{Mat}_n(y) =: Y.$$

(iv) Calculate

$$X = A_0^*UR,$$

and get x_i as the i-th column of X.

The Sylvester type equation in (iii) can efficiently be solved by methods provided in [8].

6. Some remarks about efficiency

Now the costs of the three approaches "normal equation" (6), STR and STR-C will be compared. We start from matrices $A_i \in \mathbb{R}^{n\times N}$ and T time steps.

According to [7] the direct solution of a $n \times n$ system needs $2n^3/3$ FLOPS. According to [8] the costs for the solution of the Sylvester type equation in procedure

STR-C can be bounded by $25(n+T)^3$ FLOPS. The step (iv) in STR and STR-C needs $2Tn(T+N)$ FLOPS in each case.

If we assume $n = 64, N = 5000, T = 100$, we get

- a total cost of $2/3(NT)^3$ FLOPS, if we use the normal equation approach. Considering the given numbers, this is $8.3 \cdot 10^{16}$ FLOPS.
- a total cost of $2/3(nT)^3 + 2Tn(T+N)$ FLOPS in the case of procedure STR. Based on the numbers given above, this is an amount of $1.75 \cdot 10^{11}$ FLOPS.
- a total cost bounded by $25(n+T)^3 + 2Tn(T+N)$ FLOPS for the procedure STR-C, which makes $1.76 \cdot 10^8$ FLOPS.

So we see, that the procedures STR and STR-C are really efficient compared to the "naive" normal equation approach.

7. Regularization properties of the procedure STR

As the solution x provided by the procedure STR depends on λ and μ, it can be written as $x = x_{ST}(\lambda, \mu)$. In the following, the processes $\mu \to 0$ and $\mu \to \infty$ will be considered. One additional assumption is $t_{i+1} = t_i + 1$ for all i, so that D has only entries 1 and -1. Other constant increments can be put into the parameter μ.

Now matrix $R^\infty = R^\infty(\lambda/\mu) = R^\infty(\rho)$ will be analyzed.

Before we start we need the following lemma. See, e.g. [9]:

Lemma 7.1 In the case of $t_{i+1} - t_i = 1$ the Matrix $DD^\top \in \mathbb{R}^{(T-1)\times(T-1)}$ has normed eigenvectors u_μ with

$$(u_\mu)_\nu = \sqrt{\frac{2}{T}} \sin\left(\frac{\nu\mu\pi}{T}\right) \qquad 1 \le \mu, \nu \le T-1$$

and corresponding eigenvalues

$$\lambda_\mu = 4\sin^2\left(\frac{\mu\pi}{2T}\right) \qquad 1 \le \mu \le T-1.$$

Theorem 7.2 We have

$$\lim_{\rho\to\infty} R^\infty(\rho) = (\delta_{i,j})_{i,j}$$

and

$$\lim_{\rho\to 0} R^\infty(\rho) = \left(\frac{1}{T}\right)_{i,j}.$$

Proof: It is $R^\infty(\rho) = I_T - D^\top(DD^\top + \rho^2 I_{T-1})^{-1}D$. Thus, the first statement follows from

$$(DD^\top + \rho^2 I_{T-1})^{-1} = \rho^{-2}(\rho^{-2}DD^\top + I_{T-1})^{-1}.$$

Due to Lemma 7.1 the eigenvalues of $DD^\top$ do not vanish, so the matrix $DD^\top$ is regular. Thus, we consider

$$M := \lim_{\rho\to 0} R^\infty(\rho) = I_T - D^\top(DD^\top)^{-1}D. \tag{18}$$

The matrix M has the properties $MD^\top = DM = 0$, thus $m_{i,j} = m_{i,j+1}$ and $m_{i,j} = m_{i+1,j}$. So we can conclude that M is a matrix with constant entries. In

order to calculate this entry, we analyze $(D^\top X D)_{1,1}$ with $X = (DD^\top)^{-1}$. Due to Lemma 7.1, X can be written as

$$X = \sum_{\mu=1}^{T-1} \lambda_\mu^{-1} u_\mu u_\mu^\top.$$

If we consider $(D^\top X D)_{1,1} = x_{1,1} - x_{1,2} - x_{2,1} + x_{2,2}$ together with Lemma 7.1 and the representation of X given above, we get

$$(D^\top X D)_{1,1} = \frac{1}{2T} \sum_{\mu=1}^{T-1} \left(\frac{\sin\left(\frac{\mu\pi}{T}\right) \sin\left(\frac{\mu\pi}{T}\right)}{\sin^2\left(\frac{\mu\pi}{2T}\right)} - 2\frac{\sin\left(\frac{\mu\pi}{T}\right) \sin\left(\frac{2\mu\pi}{T}\right)}{\sin^2\left(\frac{\mu\pi}{2T}\right)} + \frac{\sin\left(\frac{2\mu\pi}{T}\right) \sin\left(\frac{2\mu\pi}{T}\right)}{\sin^2\left(\frac{\mu\pi}{2T}\right)} \right).$$

If we write the sin function in terms of exponential functions, and if $x^2 - y^2 = (x+y)(x-y)$ is applied successively, we arrive at

$$(D^\top X D)_{1,1} = \frac{T-1}{T}.$$

Together with (18) one gets

$$(M)_{1,1} = 1 - \frac{T-1}{T} = \frac{1}{T},$$

which proves the second statement of the theorem.

■

For further interpretations of the limits of $x_{ST}(\lambda, \mu)$, two operators describing the temporal uncoupled problem and the static problem according to the linear operators A_i are introduced.

The operators are

$$A_{static} = \begin{bmatrix} A_1 \\ \vdots \\ A_T \end{bmatrix} \quad \text{and} \quad A_{uncoupled} = \begin{bmatrix} A_1 & & \\ & \ddots & \\ & & A_T \end{bmatrix}.$$

Then solving $A_{static} x = m$ provides the static solution $x \in H$ of $A_i x = m_i$ for all i , and solving $A_{uncoupled} x = m$ provides the temporal uncoupled solution $x = (x_i)_i \in H^T$ of $A_i x_i = y_i$ for all i.

First $\lim_{\mu \to \infty} x_{ST}(\lambda, \mu)$ will be analyzed. Due to Theorem 7.2 and step (iii) of STR we get u by solving

$$\left(\left[\frac{1}{T} A_i A_j^* \right] + \lambda^2 I \right) u = y,$$

which is the same as

$$\left(\frac{1}{T} A_{static} A_{static}^* + \lambda^2 I \right) u = y.$$

If we set $v = u/T$ this is equivalent to

$$\left(A_{static} A_{static}^* + \lambda^2 T I \right) v = y.$$

The last step in procedure STR delivers a vector x_{ST} with T constant entries

$$x_k = \sum_j \frac{1}{T} A_j^* u_j = A_{static}^* v \qquad 1 \le k \le T.$$

For stating the next theorem the Tikhonov-Phillips operator

$$T_{\lambda,mode}y = \text{minarg}\left\{\|A_{mode}x - y\|^2 + \lambda^2\|x\|^2\right\} \qquad mode \in \{static, uncoupled\}$$
$$= A^*_{mode}\left(A_{mode}A^*_{mode} + \lambda^2 I\right)^{-1} y$$

and the projections

$$P_k(x_1, \ldots, x_T) = x_k \qquad 1 \le k \le T$$

are introduced. The projections are needed, because x_{ST} is a vector of size T with constant entries.

Theorem 7.3

$$\lim_{\mu\to\infty} P_k(x_{ST}(\lambda,\mu)) = T_{\lambda\sqrt{T},static}\, y \qquad 1 \le k \le T$$
$$\lim_{\lambda\to 0}\lim_{\mu\to\infty} P_k(x_{ST}(\lambda,\mu)) = A^\dagger_{static}\, y \qquad 1 \le k \le T$$

Proof: The first statement was proven above. The second statement follows from regularization properties of the Tikhonov-Phillips operator, see [10, 11]. ■

Now $\lim_{\mu\to 0} x_{ST}(\lambda,\mu)$ is studied. Again, Theorem 7.2 shows that step (iii) in STR is equivalent to solving

$$(A_iA_i^* + \lambda^2 I)\, u_i = y_i \quad \text{for all } i$$

and x is calculated by

$$x_i = A_i^*\, u_i \quad \text{for all } i$$

These two steps can be written as

$$(A_{uncoupled}A^*_{uncoupled} + \lambda^2 I)\, u = y,$$

followed by

$$x = A^*_{uncoupled}u.$$

So we get

Theorem 7.4

$$\lim_{\mu\to 0} x_{ST}(\lambda,\mu) = T_{\lambda,uncoupled}\, y$$
$$\lim_{\lambda\to 0}\lim_{\mu\to 0} x_{ST}(\lambda,\mu) = A^\dagger_{uncoupled}\, y$$

Proof: Again, the first statement is proven above. The prove of the second statement is done in the same way as in the proof of Theorem 7.3. ■

So, one can say, that procedure STR delivers regularizations of the static as well as the uncoupled problem, depending on the limiting process of the temporal regularization parameter μ. STR produces a balance between the two extremes "static" and "uncoupled".

One last remark: The limiting processes in Theorems 7.3 and 7.4 can not be done in an arbitrary way. For example if we proceed $(\lambda,\mu) \to (0,0)$ by $(\lambda_i,\mu_i) = (\alpha/i, 1/i)$, we get the matrix $R^\infty(\lambda_i/\mu_i) = R^\infty(\alpha)$ and the result of the procedure STR does not converge to $A^\dagger_{static}\, y$ or $A^\dagger_{uncoupled}\, y$.

Acknowledgments

This work was supported by the German ministry of education and research (03-LO7SA2-2, 03-BU7AA1-4).

References

[1] U. Schmitt, A.K. Louis, F. Darvas, H. Buchner, and M. Fuchs. Numerical Aspects of spatio-temporal Current Density Reconstruction from EEG-/MEG-Data. *IEEE Trans Med Imag*, 20(4):314–324, 2001.

[2] M. Vauhkonen and P.A. Karjalainen. A Kalman Filter Approach to track fast Impedance Changes in electrical Impedance Tomography. *IEEE Trans. Biomed. Eng.*, 45(4):486–493, 1989.

[3] A. Seppänen, M. Vauhkonen, E. Somersalo, and J.P. Kaipio. State Space Models in Process Tomography - Approximation of state Noise Covariance. *Inv Probl Eng*, in press, 2000.

[4] R.A. Williams and M.S. Beck. *Process Tomography, Principles, Techniques and Applications.* Butterworth-Heinemann Ltd, Oxford, 1995.

[5] D.H. Brooks, G.F. Ahmad, and R.S. MacLeod an G.M Maratos. Inverse Electrocardiography by simultaneous Imposition of multiple Constraints. *IEEE Trans Biomed Eng*, 46(1):3–17, 1999.

[6] M.S. Grewal and A.P. Andrews, Kalman FIltering. Prentice Hall, 1993.

[7] G.H. Golub and C.F. van Loan. *Matrix Computations.* John Hopkins University Press, 3rd edition, 1996.

[8] J.D. Gardiner, A.J. Laub, J.J. Amato, and C.B. Moler. Solution of the Sylvester Matrix Equation $AXB^\top + CXD^\top = E$. *ACM Transactions on Mathematical Software*, 18(2):223–238, 1992.

[9] G.D. Smith. *Numerische Lösung von partiellen Differentialgleichungen.* Vieweg, 1970.

[10] A.K. Louis. *Inverse und schlecht gestellte Probleme.* Teubner, Stuttgart, 1989.

[11] D. Colton and R. Kress. *Inverse acoustic and electromagnetic scattering theory.* Springer, 1992.

Efficient Algorithms for the Regularization of dynamic inverse Problems – Part II: Applications

U Schmitt⋆, AK Louis⋆, C Wolters†,‡ and M Vauhkonen♯

⋆ Institute for Applied Mathematics, P.O. Box 151150, Saarland University, 66041 Saarbrücken, Germany.
† Max-Planck Institute for Mathematics in the Sciences, Inselstr. 22, 04103 Leipzig, Germany.
‡ Max-Planck Institute of Cognitive Neuroscience, PO Box 500355, 04303 Leipzig, Germany.
♯ Department of Applied Physics, University of Kuopio, PO Box 1627, 70211, Kuopio, Finland.

E-mail: schmitt@num.uni-sb.de

Abstract. In the first part of this paper the notion of dynamic inverse problems was introduced and two procedures, namely STR and STR-C, for the efficient spatio-temporal regularization of such problems were developed.

In this part the application of the new methods to three practical important problems, namely dynamic computerized tomography, dynamic electrical impedance tomography and spatio-temporal current density reconstructions will be presented. Dynamic reconstructions will be carried out in simulated objects which show the quality of the methods and the efficiency of the solution process. A comparison to a Kalman-smoother approach will be given for dynEIT.

Submitted to: *Inverse Problems*

AMS classification scheme numbers: 34A55, 49N45

1. Introduction

In the first part [1] of this paper we introduced the notion of dynamic inverse problems and developed two efficient procedures for spatio-temporal regularization, namely STR and STR-C. We will now give a brief repetition of the key facts appearing in the first part.

Starting point is a measuring procedure which needs a certain amount of time. During this time span, measurements are taken at time steps t_i. A dynamic problem is then described by equations $A_i\, x_i = y_i$, where i is a temporal index, i.e. , the linear operator A_i maps the properties x_i of an investigated object to the measurements y_i at time step t_i.

Since the operators A_i are under-determined in most cases, the degree of freedom in $A_i\, x_i = y_i$ is very high. Due to this fact, and due to the ill-posedness of these equations, we consider the *a priori* information "temporal smoothness" which is introduced as follows: in order to achieve a solution with the desired properties we

expand the well known Tikhonov-Phillips minimization task with an additional term which measures the total variance of the x_i. Thus, we solve

$$\Phi(x) = \sum_{i=1}^{T} \|A_i x_i - y_i\|^2 + \lambda^2 \sum_{i=1}^{T} \|x_i\|^2 + \mu^2 \sum_i \frac{\|x_{i+1} - x_i\|^2}{(t_{i+1} - t_i)^2} \to \min . \quad (1)$$

If we introduce

$$D = \begin{pmatrix} \frac{1}{t_2 - t_1} & -\frac{1}{t_2 - t_1} & & \\ & \frac{1}{t_3 - t_2} & -\frac{1}{t_3 - t_2} & \\ & & \ddots & \ddots \\ & & & \frac{1}{t_T - t_{T-1}} & -\frac{1}{t_T - t_{T-1}} \end{pmatrix} \in \mathbb{R}^{T \times (T-1)},$$

the efficient solution of this minimization task is given by the following procedure named STR [1]:

(i) **Input**: data y, spatial regularization parameter λ, temporal regularization parameter μ.

(ii) Calculate Q and R

$$Q = \left(DD^\top + \frac{\lambda^2}{\mu^2} I_{T-1} \right)^{-1}$$
$$R = I_T - D^\top Q D = (r_{i,j})_{i,j}.$$

(iii) C is defined by

$$C = [r_{i,j} A_i A_j^*]_{i,j}.$$

(iv) Solve

$$(C + \lambda^2 I_{G_1 \oplus \cdots \oplus G_T})\, u = y.$$

(v) Finally the x_i are calculated by

$$x_i = \sum_j r_{i,j}\, A_j^* u_j.$$

In order to achieve efficiency, in a first step one calculates $A_j^* u_j$ for each j and afterwards x_i.

As this procedure is formulated in terms of operator equations, which may map between infinite dimensional spaces, one needs a discretization scheme for their numerical solution. See [1] for further information.

If the linear operators A_i are identical for all time steps and if these operators are matrices, one can enhance the efficiency by using the following procedure STR-C:

(i) **Input**: data y, spatial regularization parameter λ, temporal regularization parameter μ.

(ii) Calculate Q and R according to

$$Q = \left(DD^\top + \frac{\lambda^2}{\mu^2} I_{T-1} \right)^{-1}$$
$$R = I_T - D^\top Q D.$$

(iii) Solve the generalized Sylvester equation

$$(A_0 A_0^*) U R + \lambda^2 U = \mathrm{Mat}_n(y) =: Y.$$

(iv) Calculate

$$X = A_0^* U R,$$

and get x_i as the i-th column of X.

The equation in step (iii) is an equation of Sylvester type, an efficient solution algorithm can be found in [2].

2. Dynamic computerized tomography

In the following the problem of dynamic computerized tomography (dynCT) will be studied. We will describe how procedure STR can be applied and some numerical tests will be carried out. An overview of the mathematics of computerized tomography can be found in [3, 4, 5].

2.1. Application of procedure STR

dynCT is a linear problem which will be formulated as operator equations between infinite dimensional Hilbert spaces.

We consider *parallel geometry*, i.e., the forward problem is described as follows: First

$$L(s,\omega) = \{x \in \mathbb{R}^2 \mid s - x \cdot \omega = 0\} \qquad \omega \in S^1, s \geq 0$$

is defined. Thus, L is a line orthogonal to ω with distance s to the origin. The *Radon transform* $\mathcal{R}$ is then defined by

$$\mathcal{R} : L^2(\Omega) \to L^2([-1,1], S^1)$$
$$\mathcal{R}f(s,\omega) = \int_{L(s,\omega)} f(x)\,\mathrm{d}x = \int_\Omega \delta(s - x\cdot\omega) f(x)\,\mathrm{d}x$$

and

$$\mathcal{R}_i f(s) = \mathcal{R}_{\theta_i} f(s) = \mathcal{R}f(s,\omega_i)$$

according to $\omega_i = (-\sin\theta_i, \cos\theta_i)^\top$, $1 \leq i \leq T$, and $\Omega = \{x \mid \|x\| \leq 1\}$. We assume that the θ_i are equidistant, $0 \leq \theta_i < 2\pi$. So $\mathcal{R}_i$ maps the density f_i of the scanned object at a time t_i to the measurements at this point of time. Due to the variation of θ during a fixed period of time, we get a dynamic problem.

In order to apply the procedure STR to this problem, we have to determine the weights $r_{i,j}$ as described in step (ii) of STR. As the angles are equispaced, we assume

$$D = \begin{pmatrix} 1 & -1 & & & \\ & 1 & -1 & & \\ & & \ddots & \ddots & \\ & & & 1 & -1 \end{pmatrix}$$

Now, $R = (r_{i,j})$ can be computed as described in step (ii) of STR.

Then, we have to consider the operator

$$C = [r_{i,j} A_i A_j^*]$$

with $A_i = \mathcal{R}_{\theta_i} = \mathcal{R}_i$. So C maps from $\left(L^2([-1,1])\right)^T$ to itself. It is easy to show that

$$\mathcal{R}_i^* g(x) = g(x \cdot \omega_i).$$

That is, $\mathcal{R}_i^*$ extends the function g on the detector to a function on the object Ω, such that $\mathcal{R}_i^* g$ is constant along lines $L(s, \omega_i)$. Due to geometric invariances of the Radon transform [4] we have

$$\mathcal{R}_i \mathcal{R}_j^* = \mathcal{R}_{(i-j) \bmod T} \mathcal{R}_0^*$$

and if we define

$$C_i = \mathcal{R}_i \mathcal{R}_0^*$$

$[C]$ can be written as

$$[C] = [r_{i,j} C_{(i-j) \bmod T}] \tag{2}$$

If we want to solve step (iv) in STR numerically by a projection scheme, we discretize the C_i and weight and compound the emerging matrices according to Lemma 4.1 and (2) to a discretization of $[C]$.

For the discretization of C_i we start from angles

$$\theta_i = 2\pi \frac{i-1}{T}, 1 \le i \le T$$

and N detector elements at

$$s_j = \frac{2j - 1 - N}{N - 1}$$

such that $s_1 = -1$ and $s_N = 1$. If we now use pointwise linear basic functions ϕ_k on the detector, defined by $\phi_k(s_j) = \delta_{j,k}$ and point collocations $\psi_k = \delta_{s_k}$, we get a discrete version $\tilde{C}_i \in \mathbb{R}^{N \times N}$ of C_i by

$$(\tilde{C}_i)_{j,l} = \psi_j C_i \phi_l = (\mathcal{R}_i \mathcal{R}_0^* \phi_l)(s_j).$$

That is, one has to extend the "hat"-function ϕ_i to the object Ω, such that the extension is constant along lines parallel to the x-axis. Next, one has to calculate the line integral of this function along the line $L(s_j, \omega_i)$. See figure 1. In detail: first, we have to calculate the points

$$p_1 = L(s_{l-1}, \omega_0) \cap L(s_k, \omega_i) \quad p_2 = L(s_l, \omega_0) \cap L(s_k, \omega_i) \quad p_3 = L(s_{l+1}, \omega_0) \cap L(s_k, \omega_i). \tag{3}$$

Then, we determine linear functions α_i such that

$$\alpha_1(p_1) = 0 \qquad \alpha_1(p_2) = 1 \qquad \alpha_2(p_2) = 1 \qquad \alpha_2(p_3) = 0.$$

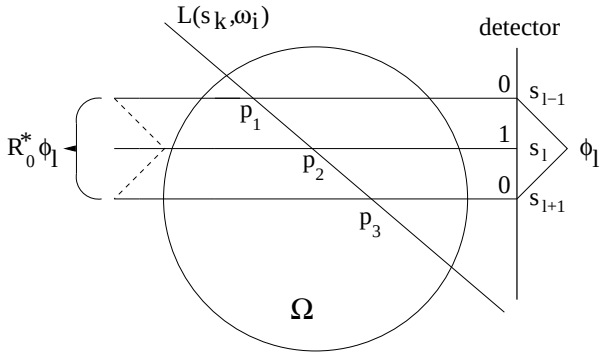

Figure 1. Calculation of the entries of $\tilde{C}_i$

Now

$$(\tilde{C}_i)_{k,l} = \int_{p_1}^{p_2} \alpha_1(x)\,dx + \int_{p_2}^{p_3} \alpha_2(x)\,dx.$$

Further, we have to consider several subcases: the points p_i may be outside the object, the points p_i may not exist, or the linecuts in (3) may be whole lines, not just points. These are technical details which are handled accordingly.

Step (iv) of STR now delivers vectors u_i and corresponding piece wise linear functions $\tilde{u}_i = \sum_j (u_i)_j \phi_j$.

In order to complete the implementation of STR we have to compute step (v) as follows. First we divide $[-1,1]$ into n points $z_i = \frac{2i-n-1}{n-1}$, such that $z_1 = -1$ and $z_n = 1$. Then we construct a grid G_n by

$$G_n = \{(z_i, z_j) \mid 1 \le i,j \le n\}$$

The resulting dynamical solutions f_i of $\mathcal{R}_i f_i = g_i$ will be computed according to step (v) of STR in points $p \in G_n \cap \Omega$ by

$$f_i(p) = \sum_j r_{i,j}(R_j^* \tilde{u}_j)(p) = \sum_j r_{i,j} \tilde{u}_j(p \cdot \omega_j).$$

In order to evaluate this formula in an efficient way, we first compute functions U_j on G_n by

$$U_j(p) = \tilde{u}_j(p \cdot \omega_j)$$

and then compute the sum

$$f_i(p) = \sum_j r_{i,j} U_j(p).$$

To summarize, we get the following algorithm

(i) **Input**: data g, spatial regularization parameter λ, temporal regularization parameter μ.

(ii) Starting with D, λ, μ compute Q, R according to

$$Q = \left(DD^\top + \frac{\lambda^2}{\mu^2} I_{T-1} \right)^{-1}$$
$$R = I_T - D^\top Q D = (r_{i,j})_{i,j}.$$

(iii) Compute matrices $(\tilde{C}_i)_{j,l} = \psi_j C_i \phi_l = (\mathcal{R}_i \mathcal{R}_0^* \phi_l)(s_j)$. Then, $\tilde{C}$ is compounded according to

$$\tilde{C} = (r_{i,j} \tilde{C}_{(i-j) \bmod T}) \in \mathbb{R}^{NT \times NT}.$$

(iv) Solve

$$(\tilde{C} + \lambda^2 I_{NT})\, u = g.$$

with $u = (u_1^\top, \ldots, u_T^\top)^\top$ and $g = (g_1^\top, \ldots, g_T^\top)^\top$.

(v) Discretize $[-1,1]^2$ using a grid G_n and compute

$$U_j(p) = \begin{cases} \tilde{u}_j(p \cdot \omega_j) & \text{if } p \in \Omega \cap G_n, \\ 0 & \text{else.} \end{cases}$$

Compute $\tilde{u}_j(s)$ by linear interpolation of u_j.
Finally, the solution of dynCT is achieved by

$$f_i(p) = \sum_j r_{i,j}^\infty U_j(p)$$

with $p \in G_n$.

Step (iv) in this procedure corresponds to a linear system on the detector and step (v) is a weighted and discrete version of the backprojection $\mathcal{R}^\sharp \tilde{u}_j$, see [5, 4].

If we had used step wise constant functions on the detector and functionals

$$\psi_l(f) = \int_{s_{l-1/2}}^{s_{l+1/2}} f(x) \mathrm{d}x,$$

we would have got a dynamic version of the *direct algebraic method* as proposed in [4].

2.2. Numerical Tests

We will see two numerical tests based on the procedure STR applied to dynCT.

The design parameters are as follows: We used a 300×300 grid for reconstruction, that is $n = 300$. Further, we had 87 angular positions, which means we considered $T = 87$ time steps. The detector is divided into 81 points, which means $N = 81$. We determined $\lambda = 0.01$ and $\mu = 1.0$ by experimentation. The data were generated analytically, no noise was added.

The two dynamic objects, that will be studied, have the same structure, see figure 2. The circular objects are static and the emphasized ellipse is dynamic.

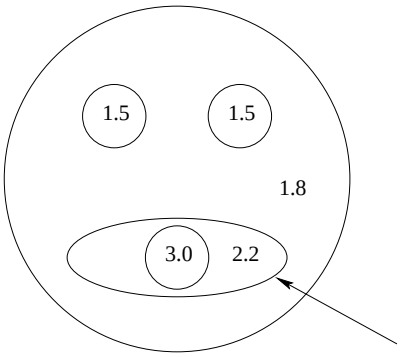

Figure 2. The structure of the considered dynamic objects. The numbers describe the density of the objects, the highlighted ellipse is the dynamic part of the object.

2.2.1. First Example The first example considers the case of slight patient motion: the examined organs behave statically up to time step 44 and the ellipse lies on the right side. Then, from time step 45 on, the ellipse lies on the left side, the other organs do not move. The object and the according reconstructions are shown in figure 3. At

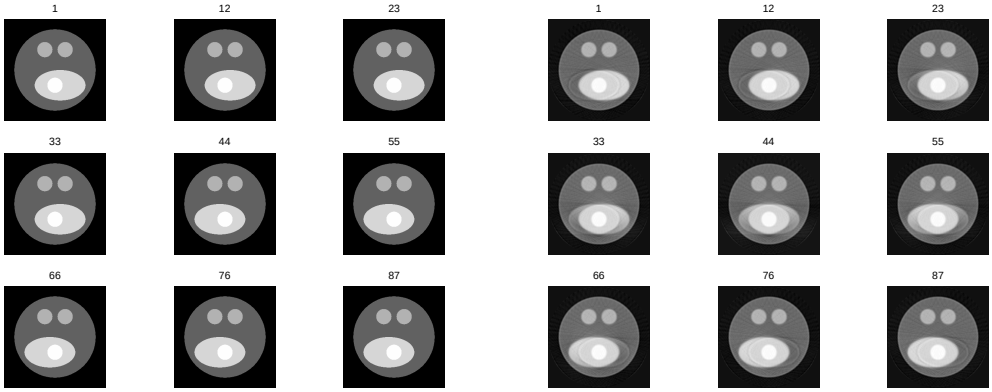

Figure 3. Dynamic object number one and reconstructions. In the left part one can see the original dynamic object, in the right part the reconstructions are depicted. The numbers above the single pictures are the corresponding time steps.

the beginning and at the end of the scanning process the quality of the reconstruction is quite good, in the neighborhood of timestep 43 the reconstructions are blurred and show slight artifacts. Nevertheless one can see the underlying dynamics.

2.2.2. Second Example In this case we examine a dynamic object where the size of the ellipse increases from time step one to time step 87. This corresponds to a CT at the human heart or to a CT of the lung during inhalation. The object and the according reconstructions can be seen in figure 4.

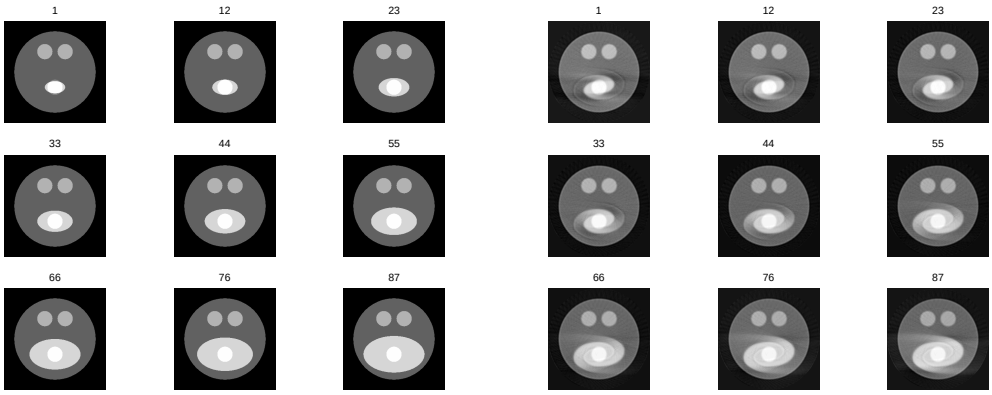

Figure 4. Dynamic object number two and reconstructions. In the left part one can see the original dynamic object, in the right part the reconstructions are depicted. The numbers above the single pictures are the corresponding time steps.

2.2.3. Discussion As we have seen the described method is able to reveal dynamics in a scanned object. The reconstructions are afflicted with artifacts which correspond to the weak *a priori* information we considered. Nevertheless, the method is able to distinguish between pathological findings (which should appear in reconstructions belonging to all time steps) and motion artifacts (which are supposed to appear in reconstructions according to few time steps only). Reconstruction procedures which deliver only one picture do not have this property. Thus, a practical application of our method is imaginable.

3. Dynamic electrical impedance tomography

Electrical impedance tomography (EIT) tries to determine the conductivity inside a given object based on electrical measurements on the objects surface. For applications see [6, 7, 8, 9, 10]. Article [11] gives an extensive survey of EIT.

EIT is based on a non-linear ill-posed problem that can be interpreted as a dynamic problem, which we will name as dynEIT in the following. In the first section we will give some preliminaries and we will apply the procedure STR to the problem of dynEIT by linearization of the underlying problem. In a second section we will give some numerical tests which we will compare to a known procedure based on so-called (fixed interval) Kalman-smoothers.

3.1. Application of the procedure STR

The electrical measurements addressed above consist of measured voltages based on injected current patterns. Due to the variation of the currents from time step to time step, one can interpret EIT as a dynamic problem dynEIT. We assume that the time steps are equispaced.

Our calculations are based on a so-called *complete electrode model* which is proposed in [12]. The outstanding quality of this model is studied in [13]. It is formulated by the following equations

$$\begin{aligned} \operatorname{div}(\sigma \nabla u) \qquad &= 0 \end{aligned}$$

$$\begin{aligned}
\int_{e_l} \sigma \frac{\partial u}{\partial n} dS &= I_l \qquad 1 \le l \le L \\
\sigma \frac{\partial u}{\partial n}\Big|_{\partial\Omega \setminus \cup e_l} &= 0 \\
\left(u + z_l \sigma \frac{\partial u}{\partial n}\right)\Big|_{e_l} &= U_l \qquad 1 \le l \le L.
\end{aligned}$$

Here, L is the number of electrodes, I_l is the injected current at electrode e_l, U_l is the measured voltage at this electrode, σ is the conductivity distribution, u is the electrical potential inside the examined object Ω, z_l is a so-called contact impedance at electrode e_l and n is the outward normal at $\partial\Omega$.

This equation can be solved by converting it to a *variational equation* which can be solved by a finite element method (FEM), see [14, 15, 16, 13]. The uniqueness of the solution induces a non-linear operator in form of a real valued matrix

$$T : (\rho, I_l) \mapsto U$$

Here $\rho = (\rho_i)_i$ and $\sum_i \rho_i \chi_i$ is a discretized version of $\rho = 1/\sigma$. U is a vector of the measured voltages. χ_i are characteristic functions of elements Δ_i.

In order to consider EIT as a dynamic problem operators

$$A_t(\rho) = T(\rho, I_t),$$

are used which are linearized in ρ^0 as follows:

$$A_t(\rho) = A_t(\rho^0) + J_t(\rho^0)(\rho - \rho^0) + o(\|\rho - \rho^0\|)$$

The matrix $J_t(\rho^0)$ can be computed using the *stiffness matrix* of the underlying finite element method, see [14, 15, 16]. $\rho^0 \in \mathbb{R}$ can be estimated from the data according to [14, 15, 16]. In the following, ρ^0 is either a real number, or we identify ρ^0 with the vector $\rho^0(1, \ldots, 1)$. The length of this vector is arbitrary.

Starting point for the solution of dynEIT are T measurement vectors $U_i = (U_k)_i, 1 \le k \le L, 1 \le i \le T$ together with the minimization task

$$\Phi(\rho) = \|A(\rho) - U\|^2 + \lambda^2 \sum_t \|\rho - \rho^0\|^2 + \mu^2 \|B\rho\|^2 \to \min$$

with the notions

$$\begin{aligned}
\rho &= (\rho_1^\top, \ldots, \rho_T^\top)^\top \\
U &= (U_1^\top, \ldots, U_T^\top)^\top \\
A &= \operatorname{diag}(A_t) \\
B &= \begin{bmatrix} I & -I & & & \\ & I & -I & & \\ & & \ddots & \ddots & \\ & & & I & -I \end{bmatrix}
\end{aligned}$$

If we now use

$$J(\rho) = \operatorname{diag}(J_t(\rho_t))$$

and approximate A iteratively by linearization we get the following Gauß-Newton type iteration

$$\rho^{i+1} = \operatorname{minarg}_\rho \left\{ \|A(\rho^i) + J(\rho^i)(\rho - \rho^i) - U\|^2 + \lambda^2 \|\rho - \rho^0\|^2 + \mu \|B\rho\|^2 \right\}.$$

The upper indices are iteration indices. It has to be pointed out, that this minimization problem can not be tackled by the procedure STR due to the spatial regularization term $\|\rho - \rho^0\|$. If we want to use procedure STR, we have to introduce $u = \rho - \rho^0$ and $u^i = \rho^i - \rho^0$. If we consider $Bu = B\rho$ we get the iteration

$$u^{i+1} = \text{minarg}_u \left\{ \|J(\rho^i)u - (U + J(\rho^i)u^i - A(\rho^i))\|^2 + \lambda^2\|u\|^2 + \mu^2\|Bu\|^2 \right\}$$

respectively

$$\rho^{i+1} = \rho^0 + \text{minarg}_u \left\{ \|J(\rho^i)u - (U + J(\rho^i)(\rho^i - \rho^0) - A(\rho^i))\|^2 + \lambda^2\|u\|^2 + \mu^2\|Bu\|^2 \right\}.$$

This iteration has now the right mode so that STR can be applied.

3.2. Numerical Tests

For the testing of our proposed method we used synthetic data calculated by a FEM using 1968 elements for the discretization of the unit disc. Further we used $L = 16$ electrodes and $T = 16$ current patterns. For the discretization of the resistivities ρ^i we used a coarser mesh with 492 elements. The examined object is drawn in figure 5. The background has the resistivity 400Ω, the inclusions 200Ω. ρ^0 was estimated [14, 15, 16] as $\rho^0 = 396\Omega$. This object reflects the rise of a bubble in a three dimensional tube through a two dimensional plane. In the following we will compare our method with a

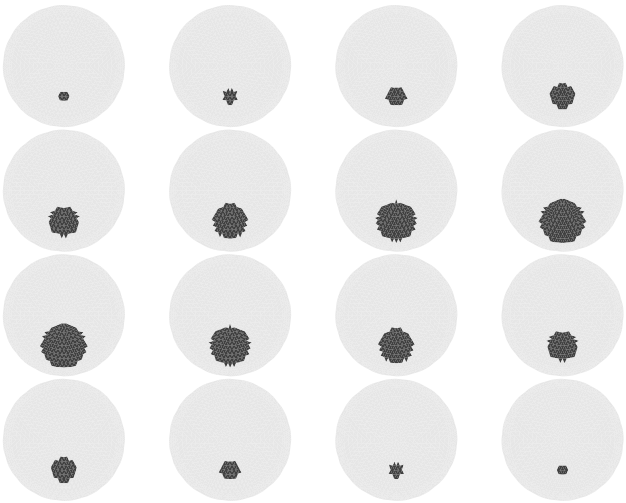

Figure 5. The examined dynamic object.

so-called (fixed interval) Kalman-smoother approach. According to [15, 17], we choose the identity matrix as regularization operator. Further details can be found in these two references. For the theory of Kalman-smoothers see [18].

It should be pointed out that in the reconstruction results the contrast was modified in order to achieve meaningful images.

3.2.1. Noiseless data We will now present three different reconstructions: our proposed method with one iteration, see figure 6, our proposed method with two iterations, see figure 7, and the Kalman-smoother method, see figure 8. All

regularization parameters where chosen by experimentation. The reconstructions of the Kalman-smoother have a slightly better quality as the reconstructions achieved by one iteration of our procedure. The quality after two iterations is again enhanced. More iterations do not result in improved reconstructions. After the precalculation of $J(\rho^0)$, the Kalman-smoother needs about 80 seconds on a Pentium-II-CPU, one iteration of our method needs about one second and two iterations need 60 seconds. The leap in the running time between one and two iterations is caused by the calculation of the linearization $J(\rho^1)$ in the second iteration of our procedure which depends on the result of the first iteration and thus can not be precalculated. The memory usage of the Kalman-smoother is about 80 times higher than the usage of our iterative method.

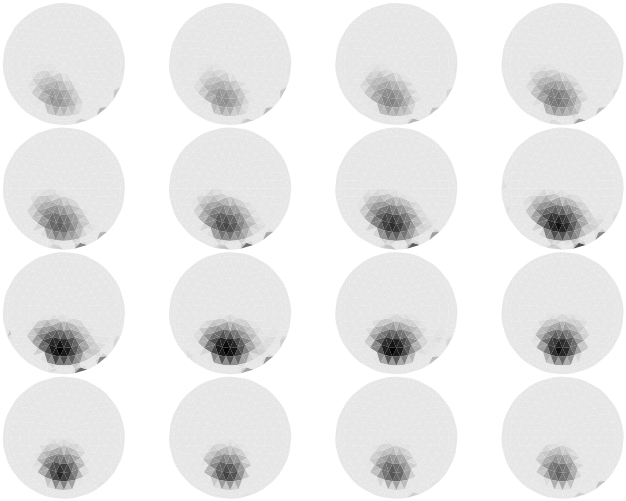

Figure 6. Reconstruction after one iteration of our procedure based on noise-free synthetic data. $\lambda = 0.001, \mu = 0.0055$.

3.2.2. Noisy data Now we superpose our synthetic data with uniform noise in the range $[-0.025 \cdot \max|U|, +0.025 \cdot \max|U|]$. The reconstructions can be seen in figures 9 and 10. Again, the Kalman-smoother reconstructions seem to have a comparable quality as the results of our approach. According to the results in 3.2.1 one further iteration of our procedure leads to slightly better reconstructions.

3.3. Discussion

We have seen that our iterative approach based on STR leads to reconstructions with a satisfying quality. The quality seams to be comparable to the quality of the reconstructions gained by the Kalman-smoother.

There is one important difference between the two approaches which has an impact on the practical use: the Kalman-smoother is controlled by three parameters, the STR approach only needs two of them. As we have already mentioned, the Kalman approach is significantly slower and has a much higher memory usage.

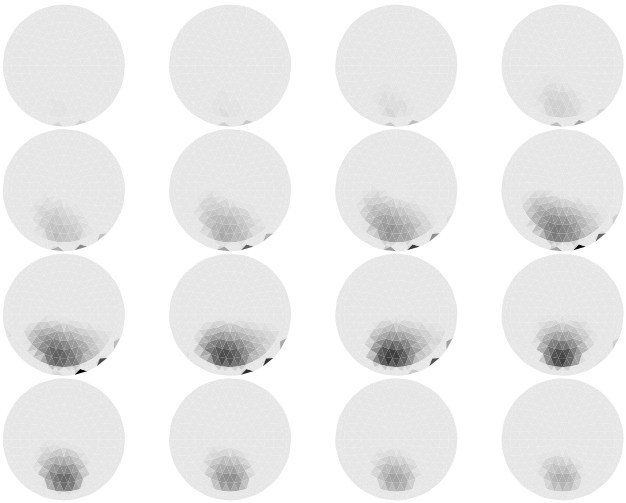

Figure 7. Reconstruction after two iterations of our procedure based on noise-free synthetic data. $\lambda = 0.014, \mu = 0.005$.

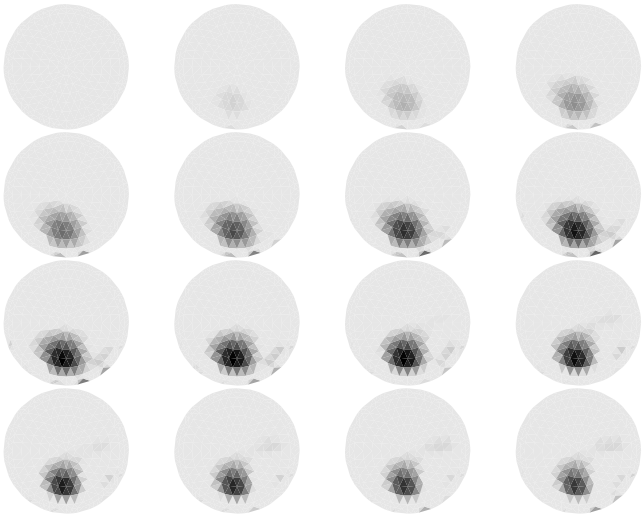

Figure 8. Kalman-smoother reconstruction based on noise-free synthetic data. According to [15, 17] we used $\alpha = 0, a_1 = 30, a_2 = 0.00001$.

It should be annotated, that there is another approach called *fixed-lag smoothing* [19] which has less memory consumption than the (fixed-interval) Kalman-smoother used here.

The *extended Kalman filter* studied in [20], is an analogue to our Gauß-Newton approach. This method is supposed to work better than the Kalman-smoother in certain cases.

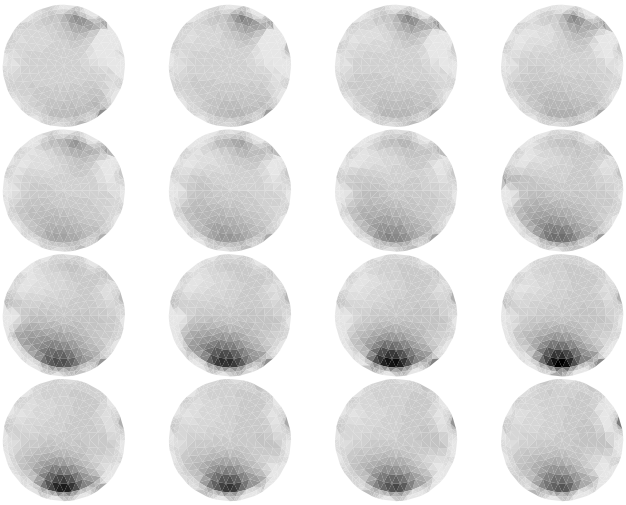

Figure 9. Reconstruction after one iteration based on noisy data. $\lambda = 0.02, \mu = 0.07$.

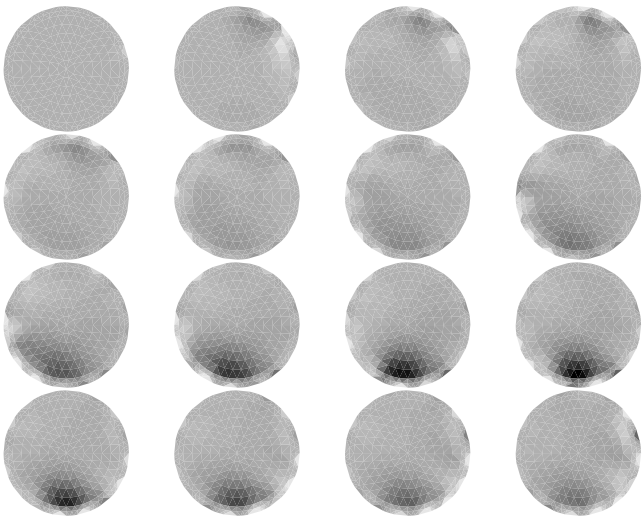

Figure 10. Kalman-smoother reconstruction based on noisy data. $\alpha = 0.08, a_1 = 30, a_2 = 0.08$.

4. Spatio-temporal current density reconstructions

Current density reconstructions (CDR) appear in the field of inverse source localizations. Here, one tries to determine electrical activity in an object by electrical measurements on the surface of the object.

One field of application is the study of neurological activity in the human brain, by means of electroencephalography (EEG) measurements on the heads surface. Focal epileptogenic discharges [21] or sources, underlying somato sensoric evoked potentials

(SEP's) can be localized [22].

An overview of the broad field applications is given in [23] and [24]. Comparable techniques can be applied to the human heart, see [25].

4.1. The forward model

The fundamental equation governing the interaction of electrical sources j and the electrical potential Φ is the Poisson equation in connection with a Neumann boundary condition

$$\begin{aligned} \operatorname{div}(\sigma \nabla \Phi) &= \operatorname{div} j \qquad \text{in} \quad \Omega \\ \langle \sigma \nabla \Phi, n \rangle &= 0 \qquad \text{at} \quad \Gamma = \partial\Omega. \end{aligned}$$

Here, σ is the conductivity tensor and the open and bounded set Ω describes the geometry of the head. n is the outward normal at $\partial\Omega$. We define $\Gamma_0 \subset \partial\Omega$ as the measurement surface. Then, the electrical measurements are obtained as $\Phi|\Gamma_0$.

In order to achieve a discrete forward model, the current in the object Ω is discretized as a fixed number of dipoles, located at points $p_i \in \Omega, 1 \leq i \leq N$, and point collocation at the measurement points are used. It is assumed that the measurements are taken at points $\xi_i \in \Gamma_0$. The set $\{p_i \,|\, 1 \leq i \leq N\}$ is called *influence space.*

If we name the kth unit vector in $\mathbb{R}^3$ as $\bar{e}_k$, and if we set $e_{i,k}$ as a dipole in p_i with moment $\bar{e}_k$, that is $e_{i,k} = \delta_{p_i} \bar{e}_k$, j can be discretized by

$$j = \sum_{i=1}^{N} \sum_{k=0}^{2} \alpha_{i+kN} e_{i,k}$$

The forward model of CDR is the so-called *leadfield matrix.* Depending on the geometrical model of the head, this matrix can be computed by analytical formulas [26, 27], boundary element methods [28] or finite element methods [29]. A fast forward solution in realistically shaped anisotropic FE head models is described in [30]. In [31] methods were described how Ω and especially tensor valued σ can be determined non-invasively and individually through multi-modal magnetic resonance imaging.

The leadfield matrix maps a current distribution j described by a vector α to the electrical measurements by $m = L\alpha$. For details see [23]. The determination of α is typical for the CDR methods in contrast to *dipole fit methods*, where only some few dipoles explaining the measured data are determined through an optimization procedure, see [32].

The data are given as functions of time, as provided by an EEG. Most existing CDR methods use separate time slices of voltage measurements without temporal coupling of neighboring time steps. Due to the physiologically motivated *a priori* information of temporal smoothness, it makes sense to use our procedures in order to achieve stability in the presence of noise. As the leadfield matrix is independent of the time, we use procedure STR-C.

4.2. A simple volume conductor model

The setup of the model is as follows: a two-dimensional influence space consisting of a 10×10 grid with a length of ten arbitrary units per side centered at $(5.5, 5.5, 0)$ is considered. Nine sensors are placed in a planar array above the grid with center at $(5.5, 5.5, 2)$, see figure 11. We use constant conductivity σ in $\mathbb{R}^3$. Thus, the leadfield

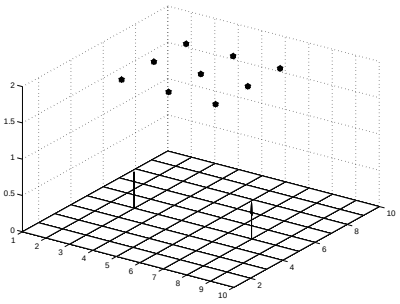

Figure 11. Sketch of the model.

matrix is obtained by

$$\begin{aligned} L_{i,j} &= \frac{1}{4\pi\sigma}\frac{r_{i,1}-p_{j,1}}{\|r_i-p_j\|^3} \\ L_{i,j+N} &= \frac{1}{4\pi\sigma}\frac{r_{i,2}-p_{j,2}}{\|r_i-p_j\|^3} \\ L_{i,j+2N} &= \frac{1}{4\pi\sigma}\frac{r_{i,3}-p_{j,3}}{\|r_i-p_j\|^3}. \end{aligned}$$

Here $r_i \in \mathbb{R}^3$ is the position of the ith sensor, $p_j \in \mathbb{R}^3$ is the position of the jth gridpoint.

Two equally oriented dipoles with moment $(0,0,1)^\top$ at $x = 3, x = 8$ both at $y = 5$ are placed on the ten by ten grid, see figure 11. A Gaussian dipole-strength time series is assigned to each dipole by

$$q(t) = q_0 \exp\left\{-\frac{(t-t_p)^2}{w^2}\right\}$$

with peaks at time slice $t_p = 5$ (dipole 1) and $t_p = 9$ (dipole 2) and a width of $w = 2.5$. See figure 12.

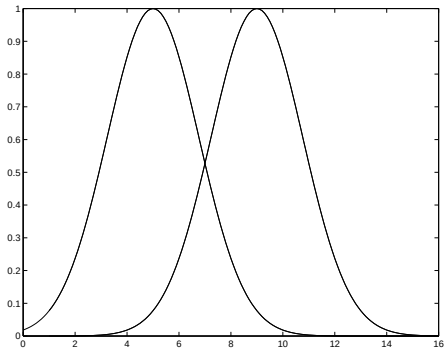

Figure 12. The activation curves of the dipoles.

4.3. Numerical Tests

In the following we will compare the results of STR-C and temporal uncoupled Tikhonov-Phillips regularizations [27]. The latter means, that j_t is computed based on

$$\alpha_t = \text{minarg}_\alpha \|L\,\alpha - y_t\|^2 + \lambda^2 \|\alpha\|^2$$

for each time step t and data $y_t, 1 \leq t \leq T$. In order to improve the signal to noise ratio for the uncoupled case, we used a Savitzky-Golay filter of order 3 and length 5, see [33, 34].

For the following reconstructions we used synthetic data which were superposed by uniform noise in the range $[-0.3 \max_t |y_t|, 0.3 \max_t |y_t|]$. This noise range is typical for EEG measurements.

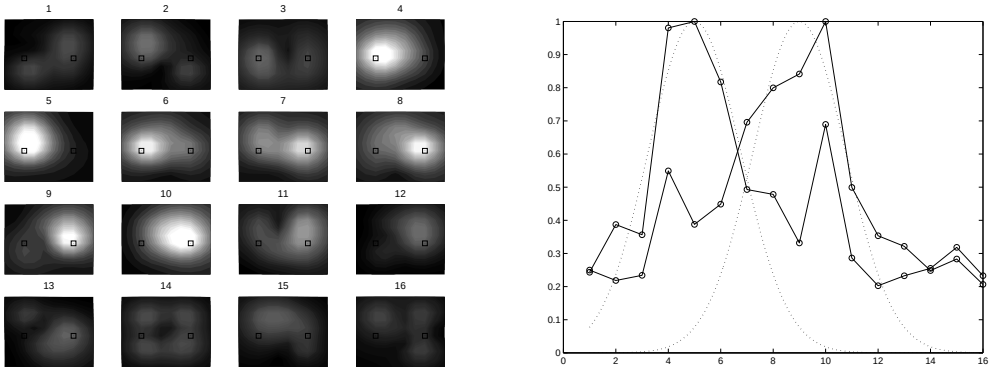

Figure 13. Temporal uncoupled reconstructions. $\lambda^2 = 2.0$.

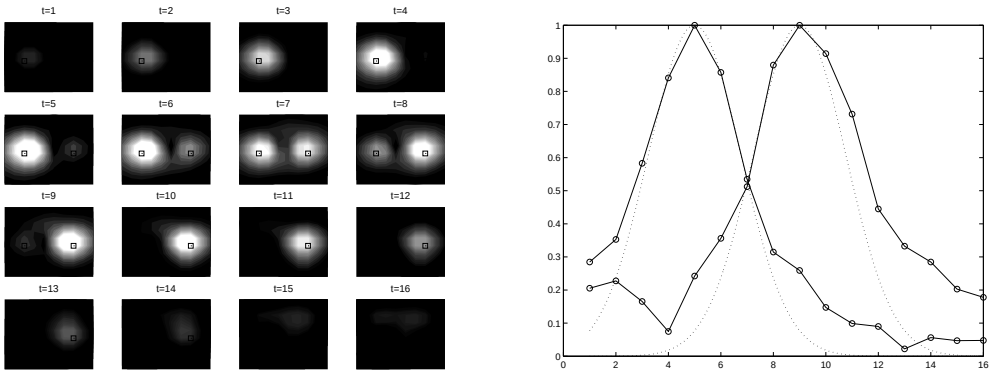

Figure 14. Reconstructions based on STR-C. $\lambda^2 = 2.0, \mu^2 = 1.5$.

In figure 13 we see the result of the temporal uncoupled Tikhonov-Phillips procedure, in figure 14 we see the result of STR-C. In the left half of these figures the current density $\|j(p,t)\|_{\mathbb{R}^3}$ for each of the 16 time steps t is shown. The small boxes mark the exact positions of the dipoles. In the right half, the reconstructed activation curves are shown.

4.4. Discussion

As one can see, our approach STR-C yields reconstructions with a smaller localization error and a more exact activation curve. Furthermore, the two dipoles are better separated. Thus, the *a priori* information of temporal smoothness leads to higher robustness against noise in the data.

For a systematic comparison of these approaches, based on an exactness measure for the localizations and a correlation measure for the activation curves, see the joint work [35].

If we compare our methods with the work of Brooks as proposed in [36], we start from the same model introducing temporal smoothness, but yield an immensely faster algorithm which has a significant impact on the clinical usability.

5. Conclusion

As shown the procedure STR is suited for the regularization of a large class of dynamic inverse problems. It was applied to dynCT which is modeled by operators between infinite dimensional spaces. Here, we could develop a procedure which is able to distinguish between pathological findings and motion artifacts.

Further dynEIT was studied, which is formulated by finite dimensional non-linear operators. Here, linearization lead to a practical algorithm. This algorithm provides reconstructions with a quality comparable to the reconstructions gained by so called Kalman-smoothers. In contrast to this Kalman approach which depends on three regularization parameters, our procedure only needs two such parameters which has an impact on the practical use of these procedures. Further our procedure is significantly faster and has less memory usage.

The last application to Electroencephalography source localization, namely stCDR, proved that the *a priori* information of temporal smoothness leads to an algorithm with higher robustness against noise than a known procedure based on temporal uncoupled Tikhonov-Phillips regularization. Further, the reconstructed peaks and the reconstructed activation curves are more accurate.

Although the used *a priori* information of temporal smoothness is quite general, STR leads in general to reconstructions which give an insight into the temporal behavior of the examined objects. In all applications the efficiency was outstanding.

Acknowledgments

This work was supported by the German ministry of education and research (03-LO7SA2-2, 03-BU7AA1-4), Prof. E. Zeidler, director of the MPI for Mathematics in the Sciences, Leipzig and by the Leipniz-Prize of the German Research Foundation awarded to Prof. A.D. Friederici, director of the MPI of Cognitive Neuroscience, Leipzig.

References

References

[1] U. Schmitt and A.K. Louis. Efficient Algorithms for the Regularization of dynamic inverse Problems - Part I: Theory. *Inverse Problems*, submitted.

[2] J.D. Gardiner, A.J. Laub, J.J. Amato, and C.B. Moler. Solution of the Sylvester Matrix Equation $AXB^\top + CXD^\top = E$. *ACM Transactions on Mathematical Software*, 18(2):223–238, 1992.

[3] G.T. Herman. *Image Reconstruction from Projections. The Fundamentals of Computerized Tomography.* Academic Press, 1980.

[4] F. Natterer. *The Mathematics of Computerized Tomography.* John Wiley & Sons, 1986.

[5] A.K. Louis. *Inverse und schlecht gestellte Probleme.* Teubner, Stuttgart, 1989.

[6] K.S. Osterman et al. Multifrequency electrical Impedance Imaging: preliminary in Vivo Experience in Breast. *Physiol. Meas.*, 21:99–109, 2000.

[7] A. Dijkstra et al. Review: Clinical Applications of electrical Impedance Tomography. *J. Med. Eng. Technol.*, 17:89–98, 1993.

[8] G. Alessandrini and L. Rondi. Stable Determination of a Crack in a planar inhomogenous Conductor. *SIAM J. Math. Anal.*, 30:326–40, 1998.

[9] A. Friedman and M. Vogelius. Determining Cracks by Boundary Measurements. *Indiana Univ. Math. J.*, 38:527–56, 1989.

[10] P.G. Kaup and M. Vogelius. Method of Imaging Corrosion Damage in thin Plates from electrostatic Data. *Inverse Problems*, 12:279–93, 1996.

[11] M. Cheney, D. Isaacson, and J.C. Newell. Electrical Impedance Tomography. *SIAM Rev.*, 41:85–101, 1999.

[12] G. Cheng, D. Isaacson, J.C. Newell, and A. Gisser. Electrode Models for electric Current computed Tomography. *IEEE Trans. Biomed. Eng.*, 36:918–24, 1989.

[13] E. Somersalo, M. Cheney, and D. Isaacson. Existence and Uniqueness for Electrode Models for electric Current computed Tomography. *SIAM J. Appl. Math*, 52:1023–40, 1992.

[14] J.P. Kaipio, V. Kolehmainen, E. Somersalo, and M. Vauhkonen. Statistical Inversion and Monte Carlo Sampling Methods in statistical Impedance Tomography. *Inverse Problems*, 16:1487–1522, 2000.

[15] M. Vauhkonen and P.A. Karjalainen. A Kalman Filter Approach to track fast Impedance Changes in electrical Impedance Tomography. *IEEE Trans. Biomed. Eng.*, 45(4):486–493, 1989.

[16] M. Vauhkonen. *Electrical Impedance Tomography and prior Information.* PhD thesis, University of Kuopio, Kuopio, Finland, 1997.

[17] J.P. Kaipio, P.A. Karjalainen, E. Somersalo, and M. Vauhkonen. State Estimation in time-varying electrical Impedance Tomography. *Annals - New York Academy of Sciences*, pages 430–439, 1999.

[18] M.S. Grewal and A.P. Andrews. *Kalman Filtering.* Prentice Hall, 1993.

[19] P.J. Vauhkonen, M. Vauhkonen, and J.P. Kaipio. Fixed-lag Smoothing and State Estimation in dynamic electrical Impedance Tomography. *Int J Numer Meth Engng*, 50:2195–2209, 2001.

[20] K.Y. Kim, B.S. Kim, M.C. Kim, Y.J. Lee, and M. Vauhkonen. Image Reconstruction in time-varying electrical Impedance Tomography based on the extended Kalman Filter. *Meas Sci Technol*, 12:1032–1039, 2001.

[21] T.D. Waberski, H. Buchner, G. Herrendorf, R. Gobbele, and W. Paulus. Properties of inverse Methods in temporal Lobe Epilepsie. *Epilepsia, in press*, 2000.

[22] H. Buchner, T.D. Waberski, and J. Noth. Generators of early cortical somatosensory evoked Potentials in Men. In Kimura and Shibasaki, editors, *Recent Advances in Clinical Neurophysiology*, pages 630–636. Elsevier Amsterdam, 1996.

[23] U. Schmitt, A.K. Louis, F. Darvas, H. Buchner, and M. Fuchs. Numerical Aspects of spatio-temporal Current Density Reconstruction from EEG-/MEG-Data. *IEEE Trans Med Imag*, 20(4):314–324, 2001.

[24] Andrä and Nowak. *Magnetism in Medicine - A Handbook.* Wiley-VCH, 1989.

[25] R.M. Gulrajani, F.A. Roberge, and P. Savard. The inverse Problem of Electrocardiography. In Macfarlane and Veitch Lawrie, editors, *Comprehensive Electrocardiology*, pages 237–288. Pergamon, 1989.

[26] R. Srebro. Continuous Current Source Inversion of evoked potential Fields in a spherical Model Head. *IEEE Trans Biomed Eng*, 42:997–1003, 1994.

[27] A.K. Louis. Parametric Reconstruction in biomagnetic Imaging. In *Inverse Problems in Scattering and Imaging*, 1992.

[28] M. Fuchs, D. Drenckhahn, H.A. Wischmann, and M. Wagner. An improved Boundary Element Method for realistic Volume-Conductor Modelling. *IEEE Trans Biomed Eng*, 45:980–997, 1998.

[29] H. Buchner, G. Knoll, M. Fuchs, A. Rienaecker, R. Beckmann, M. Wagner, J. Silny, and J. Pesch. Inverse Localization of electric Dipole Current Sources in finite Element Models of the human

Head. *Electroencephalography & Clinical Neurophysiology*, 102:267–278, 1997.

[30] A. Anwander, M. Kuhn, S. Reitzinger, and C. Wolters. A parallel algebraic Multigrid Solver for finite Element Method based Source Localization in the human Brain. *http://www.mis.mpg.de/jump/publications.html*, 2001.

[31] C. Wolters, U. Hartmann, M. Koch, F. Kruggel, S. Burkhardt, A. Basermann, D.S. Tuch, and J. Haueisen. New Methods for improved and accelerated FE Volume Conductor Modeling in EEG/MEG-Source Reconstruction. In *4th Symposion on Computer Methods in Biomech. and Biomed. Eng., Lisboa, Oct. 31.-Nov.3, 1999*, pages 489–494. Gordon and Breach, 1999.

[32] C. Wolters, R. Beckmann, A. Rienäcker, and H. Buchner. Comparing regularized and non-regularized nonlinear Dipole Fit Methods: A study in a simulated Sulcus Structure. *Brain Topography*, 12(1):3–18, 1999.

[33] A. Savitzky and M.J.E. Golay. *Analytical Chemistry*, 36:1627–1639, 1964.

[34] R.W. Hamming. *Digital Filters*. Prentice Hall, 2nd edition, 1983.

[35] F. Darvas, U. Schmitt, A.K. Louis, M. Fuchs, G. Knoll, and H. Buchner. Spatio-temporal Current Density Reconstructions (stCDR) from EEG/MEG-Data. *Brain Topography*, 13:192–208, 2001.

[36] D.H. Brooks, G.F. Ahmad, and R.S. MacLeod an G.M Maratos. Inverse Electrocardiography by simultaneous Imposition of multiple Constraints. *IEEE Trans Biomed Eng*, 46(1):3–17, 1999.